VTT Technical Research Centre of Finland

Advances in the understanding of molybdenum effect on iodine and caesium reactivity in condensed phase in the primary circuit in nuclear severe accident conditions

Gouëllo, Mélany; Hokkinen, Jouni; Kärkelä, Teemu

Published in:
Nuclear Engineering and Technology

DOI:
10.1016/j.net.2020.01.029

Published: 01/08/2020

Document Version
Publisher's final version

Nuclear Engineering and Technology 52 (2020) 1638–1649

Contents lists available at ScienceDirect

Nuclear Engineering and Technology

journal homepage: www.elsevier.com/locate/net

Original Article

Advances in the understanding of molybdenum effect on iodine and caesium reactivity in condensed phase in the primary circuit in nuclear severe accident conditions

Mélany Gouëllo*, Jouni Hokkinen, Teemu Kärkelä

VTT Technical Research Centre of Finland Ltd, P.O. Box 1000, FI-02044, VTT, Finland

ARTICLE INFO

Article history:
Received 12 June 2019
Received in revised form
20 January 2020
Accepted 28 January 2020
Available online 31 January 2020

Keywords:
Iodine transport
Molybdenum
Oxygen partial pressure
Primary circuit

ABSTRACT

In the case of a severe accident in a Light Water Reactor, the issue of late release of fission products, from the primary circuit surfaces is of particular concern due to the direct impact on the source term. CsI is the main iodine compound present in the primary circuit and can be deposited as particles or condensed species. Its chemistry can be affected by the presence of molybdenum, and can lead to the formation of gaseous iodine. The present work studied chemical reactions on the surfaces involving gaseous iodine release. CsI and MoO_3 were used to highlight the effects of carrier gas composition and oxygen partial pressure on the reactions. The results revealed a noticeable effect of the presence of molybdenum on the formation of gaseous iodine, mainly identified as molecular iodine. In addition, the oxygen partial pressure prevailing in the studied conditions was an influential parameter in the reaction.

1. Introduction

Molybdenum is present in large quantities in the fuel of a nuclear power plant, in excess relative to caesium. For instance, Fukushima Daiichi Unit-1 contained 1140 mol-Cs/core and 1850 mol of molybdenum at the time of the accident [1]. In severe accident conditions, molybdenum has been suspected to enhance the gaseous iodine fraction reaching the containment [2]. Molybdenum can be released during a core meltdown accident and particularly in large amounts in oxidizing conditions [3]. By reaction with caesium and forming stable caesium molybdates, the molybdenum would decrease the availability of caesium to form caesium iodide, and consequently, increase the gaseous iodine fraction. Due to the radiological consequences that may result from its release into the environment, iodine chemistry is particularly investigated.

Molybdenum is considered as a semi-volatile fission product and its release fraction, when heating a uranium pellet previously irradiated in a nuclear power plant to about 2400 °C, reached 50% under reducing conditions and 100% under oxidizing conditions [3]. The release of molybdenum generally begins after that of volatile fission products such as iodine and caesium. During the Phébus tests [4], keeping the FPT3 test aside, it was noticed that molybdenum underwent moderate retention in the reactor coolant system (less than 50% of released fraction was retained in the reactor coolant system [5]), similar to caesium. In the reactor coolant system, molybdenum can interact with caesium either in gaseous phase at high temperature (higher than 650 °C) or in condensed phase, once molybdenum has condensed/deposited on the surfaces.

Gaseous phase reactions that may occur in the primary circuit in nuclear accident conditions were investigated at the Institut de Radioprotection et de Sûreté Nucléaire (IRSN) [5,6]. Composition of the atmosphere where the reaction took place was found to be a determining factor in the reaction. Results of the injection of molecular iodine (I_2), caesium hydroxide (CsOH) and molybdenum trioxide (MoO_3) in oxidizing (Ar: 5.1; He: 44.1; Steam: 50.8 v/v %) and reducing conditions (Ar: 94.8; Steam: 2.39; H_2: 2.78 v/v %) in a thermal gradient tube (1600 °C–150 °C) showed a high fraction of measured gaseous iodine in the first case, while under reducing conditions almost all the iodine was in aerosol form at the outlet of the facility. When mixing molybdenum trioxide and caesium iodide (CsI) in a thermal gradient tube (1560 °C–150 °C) in oxidizing atmosphere (argon and steam (80%, v/v)), Gouëllo et al. [6] measured a percentage of gaseous iodine higher than 80% of the total amount of iodine at 150 °C when the Mo/Cs molar ratio was higher than 2.

* Corresponding author.
E-mail address: melany.gouello@vtt.fi (M. Gouëllo).

https://doi.org/10.1016/j.net.2020.01.029

The influence of molybdenum on caesium and iodine transport was also corroborated by thermodynamical calculations [7]. The study also demonstrated that for a Cs/I molar ratio of 1 and Mo/Cs molar ratio of 0.4, the proportion of gaseous iodine at 700 °C was 0.1% and reached 15% for a Mo/Cs ratio of 0.45 [7]. Following the Phébus tests, ASTEC calculations were performed [8,9]. The results showed that the molybdic acid (H_2MoO_4) would be responsible for the persistence of gaseous iodine in the reactor coolant system by the consumption of a large amount of caesium from caesium hydroxide following the reaction (1):

$$2CsOH(g) + H_2MoO_4(g) \rightarrow Cs_2MoO_4(g) + 2H_2O(g)$$

Reactions in condensed phase were studied at the Technical Research Centre of Finland (VTT). The tests were carried out on CsI/MoO_3 and CsI/Mo powder mixtures in a crucible [5,10]. The crucible was placed inside the stainless steel tube of the furnace and the furnace was heated to 650 °C under several atmospheric mixtures. The atmospheres in each test proceeded chronologically from oxidizing condition in a steam/argon mixture to more reducing conditions with increasing hydrogen fraction.

Concerning the tests performed with CsI/MoO_3, the comparison of a pure caesium iodide vaporisation test under an Ar/H_2O (94%/6%) mixture at 650 °C and a test carried out with the addition of molybdenum (molar Mo/Cs = 3) to the precursor showed an increase in the fraction of gaseous iodine from 57% to 99% of the total iodine vaporised when molybdenum was added to the caesium iodide. The results indicated the existence of reactions between molybdenum trioxide and caesium iodide in the condensed phase at 650 °C, which would lead to the formation of a substantial amount of gaseous iodine. However, the effect of steam (Ar/H_2O atmosphere) on the reaction between caesium iodide and molybdenum trioxide was not tested at 650 °C [5].

Looking at the tests performed with CsI/Mo, the influence of molybdenum presence on the release of gaseous iodine was also shown, especially in Ar/H_2O atmosphere [10].

Considering these experimental and analytical observations, the objective of the current study was to gather data on how iodine and caesium behaviour could be affected by the presence of molybdenum in severe accident conditions in the reactor coolant system. The study is specifically focused on investigating reactions, which could happen from the deposits in the reactor coolant system. One main reason has motivated the study of the reactions in condensed phase. In 1994, Sugimoto et al. [11] have reported that the deposited species in the reactor coolant system can become one of the dominant contributors to a late-phase release of the fission products. This has been observed recently. In several days after the main fission products release from the Fukushima Daiichi Nuclear Power Plant, important and unexpected delayed releases were measured [12]. One of the proposed hypothesis, which could explain the late release of iodine, would be the occurrence of chemical remobilisation from the deposits in the reactor coolant system or in the upper structure of the reactor vessel.

Since there is about 10 times more caesium than iodine released from the core during a severe accident, iodine is assumed to be released mainly as caesium iodide and the rest of the caesium as caesium hydroxide [13,14]. Reactions from caesium iodide in the deposit were then investigated.

In the gaseous phase reactions [5,6], the initial Mo/Cs molar ratio was highlighted as an important parameter involved in the release of gaseous iodine, especially for a Mo/Cs molar ratio higher than 2 [6]. In condensed phase, only initial Mo/Cs molar ratios of 5.4 for CsI/MoO_3 [5] and 8 for CsI/Mo [10] were studied at high temperature. Consequently, the present work proposed to vary the initial Mo/Cs molar ratio (Mo/Cs = 1.6; 3 and 5) and to identify how it could affect the released gaseous iodine fraction.

In parallel to this parameter, the effect of the oxygen potential prevailing in the carrier gas (oxidizing/reducing conditions) was considered. As previous tests in condensed phase between caesium iodide and molybdenum trioxide have not studied the reactions in Ar/H_2O atmosphere, it was investigated in the present work. In addition, atmosphere composed of Ar/Air is also topical in the described work. Indeed, as underlined in previous study [15], studies of fission products released from irradiated fuel heated in air are the subject of continuing multinational efforts. Separate effects tests are still required in order to reduce uncertainties and extend the experimental database for the validation of analytical models in representative conditions, notably in the primary circuit [16].

First, the effect of different initial Mo/Cs molar ratios was examined. Additionally, the effect of the oxidizing environment on the chemistry of iodine, caesium and molybdenum was investigated. The results of the tests raised the question of the initial mass of powder present in the crucible. Consequently, a test scoping the effect of the initial amount of powder was also initiated. Analysis with thermochemical equilibrium calculations was presented in the discussion section and a short comparative study was initiated between the present described results and previous results obtained at VTT under different conditions.

2. Material and methods

2.1. Experimental facility

The set-up of VTT's EXSI-PC facility used for these tests has been described in detail previously (Fig. 1) [15]. Inactive materials were used to simulate fission products. The precursor materials were in the form of powder (CsI 99.9 wt% and MoO_3 99.97 wt%, provided by Sigma-Aldrich®). The two powders were mixed in a polypropylene tube. The tube was shaken and then the mixed powders were deposited into an alumina crucible. The choice of the crucible material, non-representative of a primary circuit surface, was based on the objective of the following tests to clarify the reactions between the powdery precursor materials placed in the evaporation crucible and not with the surfaces of the crucible or primary circuit itself. Since it was previously shown that the caesium iodide precursor reacts with the iron oxide layer on the stainless steel crucible surface [17], working with an alumina crucible was preferred.

A stainless steel tube (AISI 304, inner diameter 25 mm and length 1100 mm) was pre-oxidised at 1000 °C for 3h30 in pure steam atmosphere (4.2 l/min). The evaporation crucible containing the precursor material(s) was placed inside the pre-oxidised tube, which was heated using a horizontal tube furnace (Entech ETF 30/12).

The carrier gas was fed into the heated furnace, in which the precursor materials reacted with each other and with gas. A stainless steel coupon (length 8 cm, width 1 cm) was placed at the location of the temperature gradient inside the furnace tube before the first diluter, characterized by a temperature decrease of about 100 °C due to the insulation at the outlet of the tube furnace. Reaction products were transported by the gas flow through the furnace into the primary diluter, where the sample mixture was diluted and cooled to 125 °C. The first diluter placed after the tube had the function of desaturating the gas flow and thus preventing the condensation of vapors. Argon was used as the dilution gas, and it was preheated to the set point temperature of the tube furnace. A second diluter was used to cool down the gas flow. The cooling flow passed through a porous wall structure of the diluter for preventing the retention of particles and vapors during the process. Argon at room temperature was used as the dilution gas. Next, the flow is

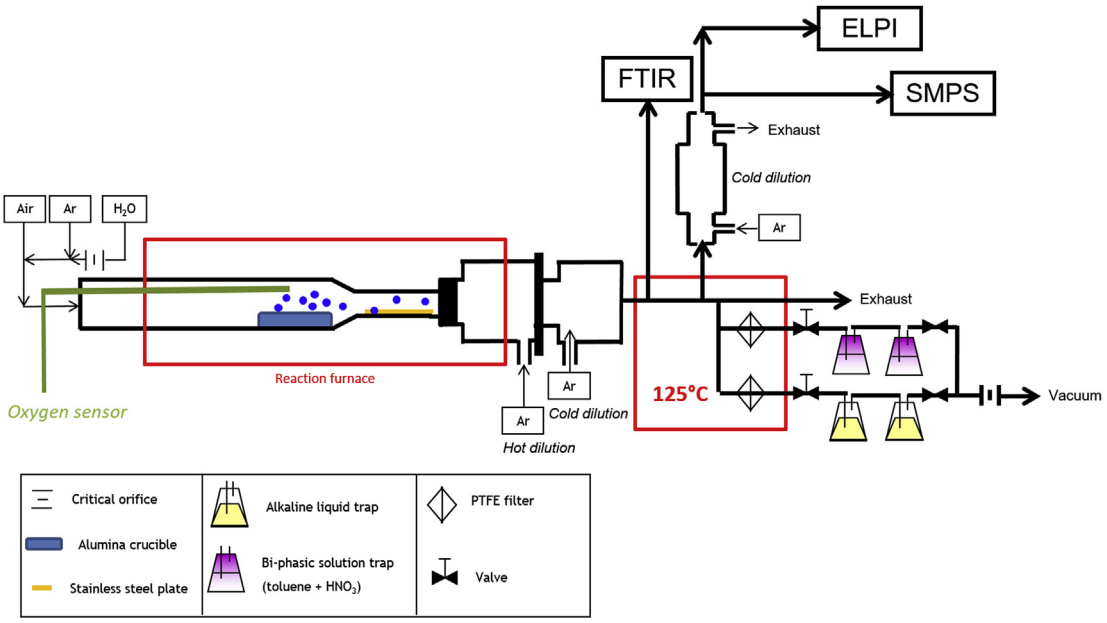

Fig. 1. Schematic figure of the experimental EXSI-PC facility.

split between the line for online aerosol measurement section and the line for elemental speciation of aerosol and gas samplings.

The sampling furnace contained two sequential sampling lines, each equipped with a polytetrafluroethylene (PTFE) membrane filter (hydrophobic, poral grade 5.0 μm, 47 mm, Mitex®) and two glass scrubbers assembled in series. The glass scrubbers contained:

- either immiscible solutions of nitric acid (HNO_3) (50 ml; pH = 2) and toluene (C_7H_8) (100 ml). This selective scrubber was used in order to trap gaseous molecular iodine (I_2) in toluene from water-soluble gaseous iodine (HI, HIO) in nitric acid aqueous phase separately in the sampling line n°1.
- or a solution of 0.1 M sodium hydroxide (NaOH) and 0.02 M sodium thiosulfate ($Na_2S_2O_3$) in water (150 ml) in the sampling line n°2.

These two sequential sampling lines aim at determining the mass transported in aerosol form (collected on the filter devices) and in gaseous form (collected in the downstream glass scrubbers).

A third line is dedicated to the on-line measurement devices for the size characterisation of suspended particles. The continuous sampling allowed to monitor the aerosol number size distributions during the experiment.

2.2. Analytical methods

The solutions and leachates from filters were analysed by Inductively Coupled Plasma Mass Spectrometry (ICP-MS). The analyses were all performed with a Thermo Fisher Scientific HR-ICP-MS Element2 apparatus. The quantification of molecular iodine in toluene was carried out by UV–visible spectroscopy using a PerkinElmer spectrophotometer model Lambda 900. In toluene, the absorption curve of molecular iodine presents two peaks at 306 nm and 497 nm, giving respective molar extinction coefficients of 7901.0 l mol^{-1} cm^{-1} and 1064.8 l mol^{-1} cm^{-1} in a 10-cm quartz cuvette. The detection limit was 1.2 ppm. Aerosol number size distributions were measured with a TSI Scanning Mobility Particle Sizer (SMPS), with series 3080 platform, series 3081 Differential Mobility Analyser (DMA) and series 3775 Condensation Particle Counter (CPC) as well as with an Electric Low-Pressure Impactor (ELPI). Steam concentration in the sample flow was monitored with a Gasmet Dx4000 Fourier Transform Infrared Spectrometer (FTIR).

Raman microspectrometry was used to study the composition of species remaining in the crucible after the test and the species deposited/condensed on the stainless steel plates. The detailed interpretation of spectra was not straightforward and was not attempted in the present work. Not having software at our disposal allowing the extraction of pure compounds, Raman microspectrometry was primarily used to compare standards to aid in the identification of unknown phases. Raman spectra were obtained with a JobinYvon® (LABRAM HR) spectrometer. The Raman backscattering was excited at 632 nm. The spectral resolution of this instrument was ~4 cm^{-1} and the spatial resolution was estimated to be ~1 μm^3.

The oxygen pressure in the inlet gas, above the crucible, was monitored with a MicroPoas probe. The MicroPoas® is a zirconia electrochemical gauge with a built-in metal reference. Unlike conventional “air reference” zirconia sensors, the MicroPoas® has its own internal reference, which is made of metal and its oxide, both placed and sealed inside a zirconia sheath. The measurement range is from 10^{-35} to 0.25 atm. The exact MicroPoas® temperature is taken into account thanks to a built-in thermocouple (K type).

2.3. Experimental matrix and procedure

The absolute pressure in the facility was fixed at 1 bar. The total gas flow rate through the reaction furnace was set at 3.8 l/min (Standard Temperature and Pressure (STP)). Two different mixtures of argon, steam, hydrogen and air have been applied in tests with the facility (see Table 1).

The volume fraction of air was chosen to be 13 vol-% in order to be comparable to the volume fraction of steam used in the previous tests (also in the current study) and to assess their influence on the gaseous iodine formation. The chosen volume fraction of air is also in accordance with the conditions in the tests of the VERCORS programme [3]. The VERCORS programme is an experimental programme composed of separate-effect tests specifically focusing on determining the source term from an irradiated fuel rod sample,

Table 1
Volume fractions of gases (vol%) in the experiments (conditions A and D).

Carrier gas composition		A	D
Gas vol%	Argon	86.7	86.7
	Steam	13.3	0
	Hydrogen	0	0
	Air	0	13.3

under conditions representative of those encountered during a severe light water reactor accident. The VERCORS HT and RT tests are particularly of interest for the current study because HT and RT tests aimed to study the transport of fission products in the primary circuit and the potential interaction of fission products with the elements composing the neutron absorbers of a Pressurized Water Reactor (PWR), and the release of low-volatile fission products. The composition of carrier gas at the end of test RT8 was 90% He + 10% Air [18]. Therefore, those conditions resemble condition D in the current study. The dry air used in the current study contains about 400 ppm of carbon dioxide (CO_2). However, based on the calculations performed with the FactSage software, the presence of CO_2 in such a low amount does not influence the iodine speciation. The flow rate of dilution gas in the first diluter was fixed to 7 and 28 l/min (STP) in the porous tube, giving a total dilution factor of 10.06 for the sampling line downstream of the two-stage dilution. A flow of 7.5 l/min (STP) was directed into the online line, and the flow rate of dilution gas in the ejector diluter for the online measurement devices was 70 l/min (STP), giving a dilution factor of 10.3 for the online sampling.

As in previous studies conducted with the EXSI-PC facility [15,19], the set-point temperature of the furnace (650 °C) was chosen so that it would be just above the melting point of caesium iodide (621 °C) and close to the hot leg temperature (700 °C) used in the Phébus FP tests [20]. However, the use of the MicroPoas probe, placed just above the crucible highlighted a temperature of the flow above the crucible of about 700 °C. Following this observation, a temperature profile was measured moving a thermocouple inside the facility for a 650 °C-set-point temperature (Fig. 2). Same observation was made: by requiring a set-point temperature of 650 °C, the temperature measured where the crucible is placed was 700 °C.

The matrix of the tests is presented in Table 2.

2.4. Theoretical analysis

Experimental results were analysed with the help of thermodynamic equilibrium calculations performed with Thermfact and GTT-Technologies FactSage 5.5. The FactSage software is the fusion of two well-known software packages in the field of computational thermochemistry: FACT-Win and ChemSage. The equilib module is the Gibbs energy minimization workhorse of FactSage. It calculates the concentrations of chemical species when specified elements or compounds react or partially react to reach a state of chemical equilibrium [21]. The coefficients of the Gibbs energy functions are tabulated in different databanks adapted to the problems to be solved; in this situation for stoichiometric solid, liquid and gaseous species. The FACT 5.3 compound database was used.

3. Results

In order to make all the measured data comparable (sequential

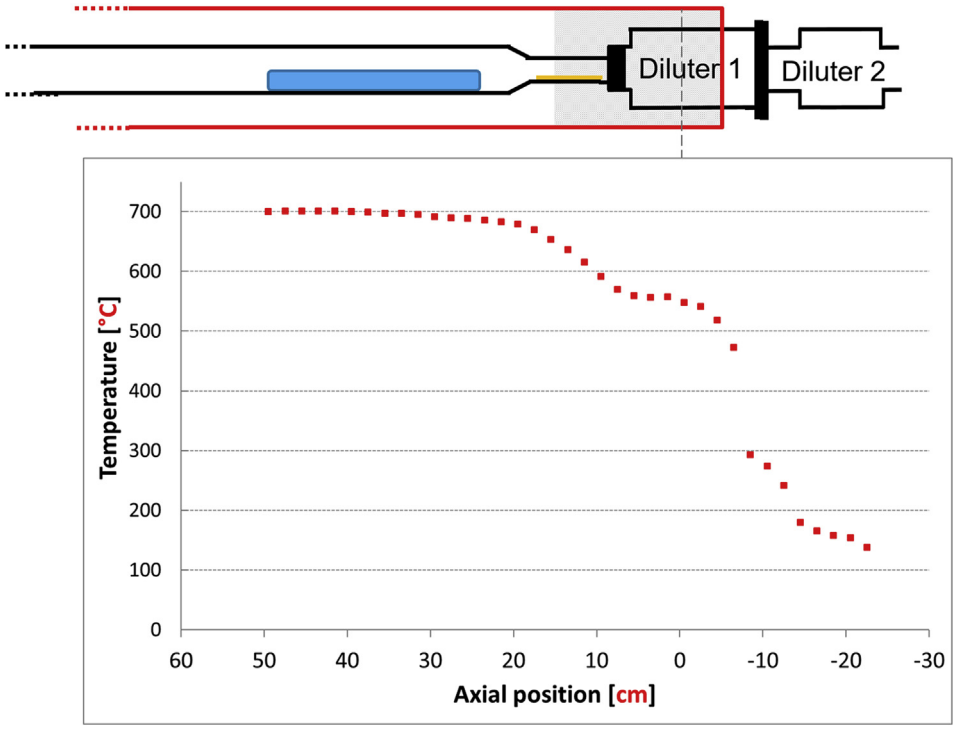

Fig. 2. The measured temperature profile inside the stainless steel tube of the furnace under Ar/H_2O atmosphere.

Table 2
Experimental matrix and test conditions. Tests CsI-A and CsI-D have already been published in Ref. [15].

Exp.	Precursor	Precursor mass [g]	Molar Mo/Cs	Carrier gas composition	Experiment duration [min]
Mo-1	CsI+ MoO_3	2.500+ 7.011	5.06	A	95
Mo-2	CsI+ MoO_3	2.500+ 7.025	5.08	D	57
Mo-3	CsI+ MoO_3	2.502+ 2.234	1.6	A	62
Mo-4	CsI+ MoO_3	2.501+ 2.235	1.6	D	62
Mo-5	CsI+ MoO_3	2.510+ 4.256	3.06	A	54
Mo-6	CsI+ MoO_3	2.504+ 4.247	3.06	D	55
Mo-7	CsI+ MoO_3	1.441+ 4.027	5.05	A	56
CsI-A	CsI	10.033	N/A	A	141
CsI-D	CsI	10.292	N/A	D	150

sampling main lines and the online measurement line), all the mass concentrations expressed in this paper were reported to the corresponding values inside the reaction furnace. So, they were systematically corrected by the dilution factor. However, it is worth to note that values correspond to the masses (aerosols or gases) that have transited inside the facility until the sampling devices and it did not take into account the percentage of deposited/condensed matter. Therefore, the mass concentrations presented in graphs correspond to the underestimated values of the real mass concentrations in the tube furnace during the vaporisation. The analysed mass concentrations on particle filter and in bubblers samples and the results obtained from on-line aerosol measurement devices are summarized in Table 3. Two successive samplings were done during each test (first sampling line n°1 then sampling line n°2). The duration of one sampling was 20 min.

3.1. Fraction of transported gaseous iodine

By comparing the amount of gaseous iodine released from the vaporisation of caesium iodide in similar atmosphere, previously published [15], the addition of molybdenum trioxide to caesium iodide distinctly increased the amount of released gaseous iodine

Table 3
Transported iodine, caesium and molybdenum mass concentrations in the experiments, calculated from the filter and bubblers samples (analysed with ICP-MS) and aerosol transport results obtained with on-line aerosol measurement devices. Results of the tests CsI-A and CsI-D have already been published in Ref. [15].

Experiment number		Mo-1	Mo-2	Mo-3	Mo-4	Mo-5	Mo-6	Mo-7	CsI-A	CsI-D
Composition of carrier gas		A	D	A	D	A	D	A	A	D
Measured $P(O_2)$ [atm] (average)		$1.17\cdot10^{-4}$	$2.76\cdot10^{-2}$	$4.72\cdot10^{-4}$	$2.76\cdot10^{-2}$	$2.24\cdot10^{-4}$	$2.72\cdot10^{-2}$	N/M[a]	N/M	N/M
Mass concentration of elements collected on filters determined by ICP-MS[b] [mg/m^3]	I	8.74	12.74	25.77	1.02	18.16	3.78	7.60	195.50	825.39
	Cs	40.14	13.88	15.23	0.52	25.89	3.25	41.47	190.49	840.27
	Mo	77.39	139.32	0.51	1.61	15.17	6.72	58.12	N/A[c]	N/A
Mass concentration of elements in the glass scrubbers determined by ICP-MS [mg/m^3]	I	18.97	69.34	145.34	200.30	18.99	56.13	33.45	21.98	40.74
	Cs	0.31	0.27	0.40	1.06	0.32	0.55	0.25	0.00	1.75
	Mo	2.41	12.89	0.24	1.93	2.22	2.06	2.10	N/A	N/A
Number of moles of iodine "I" in molecular iodine (I_2) form [mol][d]		$1.53\cdot10^{-7}$	$6.12\cdot10^{-7}$	$2.82\cdot10^{-7}$	$1.53\cdot10^{-7}$	$1.55\cdot10^{-7}$	$6.14\cdot10^{-7}$	$3.44\cdot10^{-7}$	N/M	N/M
Number of moles of iodine "I" in water-soluble form (HI or HIO) [mol][e]		$8.35\cdot10^{-8}$	$2.54\cdot10^{-7}$	$8.28\cdot10^{-8}$	$2.38\cdot10^{-8}$	$8.17\cdot10^{-8}$	$8.69\cdot10^{-8}$	$7.37\cdot10^{-8}$	N/M	N/M
Molar ratio measured on the filter	Cs/I	4.4	1.0	0.6	0.5	1.4	0.8	5.2	0.9	1.0
	Mo/Cs	2.7	13.9	0.0	4.3	0.8	2.9	1.9	N/A	N/A
Mass of residue in the crucible after the test [g]		7.089	7.162	3.198	3.522	3.017	0.376	2.079	9.436	7.863
Vaporisation rate [mg/min]		25.49	41.46	24.81	19.58	69.43	115.91	60.52	4.23	16.19
Identified compound in the crucible after the test		CsI; α-MoO_3	α-MoO_3 ?	CsI; α-MoO_3; $Cs_2Mo_3O_{10}$	unidentified	CsI; $Cs_2Mo_5O_{16}$	unidentified	CsI; α-MoO_3	CsI	CsI
ELPI [1/cm^3][f]		$4.4\cdot10^{8}$	$3.4\cdot10^{9}$	$4.3\cdot10^{4}$	$4.0\cdot10^{4}$	$2.7\cdot10^{8}$	$2.3\cdot10^{8}$	$4.5\cdot10^{8}$	$3.5\cdot10^{8}$	$1.7\cdot10^{7}$
SMPS [1/cm^3]		$1.2\cdot10^{9}$	$2.3\cdot10^{9}$	$7.5\cdot10^{4}$	$4.0\cdot10^{4}$	$8.5\cdot10^{8}$	$1.1\cdot10^{9}$	$1.4\cdot10^{9}$	$3.3\cdot10^{9}$	$9.7\cdot10^{6}$
CMD[g] [nm]		40.5	54.2	61	46.8	27.7	18.6	38.7	36	253
GSD[h]		1.5	1.43	1.8	1.6	1.3	1.2	1.4	1.5	1.4

[a] N/M: Not Measured.
[b] The mass concentration determined by ICP-MS referred to the mass collected during the whole sampling duration of line 2. The mass of element on the filter (or in glass scrubber) was measured by ICP-MS, then corrected by the dilution factor (10.06). The corrected mass concentration was divided by the sampling time (20 min) and flow rate of sampling (1.4 l/min adjusted by the computer program from temperature and pressure measured on the line).
[c] N/A: Not Applicable.
[d] Amount measured in toluene by UV–Visible spectroscopy from sampling in line 1.
[e] Amount measured in nitric acid solution by ICP-MS from sampling in line 1.
[f] The total particle number concentrations (ELPI and SMPS) presented in Table 3 are averages calculated for the duration of the test.
[g] CMD: Count Median Diameter measured by SMPS.
[h] GSD: Geometric Standard Deviation.

(Table 3). The presence of molybdenum trioxide (Mo-1) multiplied by 7 the amount of gaseous iodine (68.5%) by comparison to the reference case (CsI-A; 10.1%).

Surprisingly, the amount of gaseous iodine was higher when the initial Mo/Cs molar ratio was the lowest (i.e. 1.6). However, from a Mo/Cs molar ratio of 3–5, the amount of released gaseous iodine increased. The amount of gaseous iodine in Mo-3 is 24% higher than the amount in Mo-1. This observation was made for the two studied atmospheres.

The effect of the atmosphere composition on the release of gaseous iodine was highlighted. The presence of air in the carrier gas tended to increase the amount of gaseous iodine (Table 3), for every studied Mo/Cs molar ratio. In the Mo-2 case, the amount of gaseous iodine in presence of air represented an increase of 23% compared to the Mo-1 case.

Molecular iodine in toluene forms a complex which exhibits two absorption peaks centred at 306 nm and 498 nm [22]. These characteristic peaks were measured in all samples (Table 3) in the first glass scrubber. Molecular iodine was the main gaseous species: in steam conditions, molecular iodine represents 60–80% of the total gaseous iodine, while in air condition the molecular iodine fraction was even larger (70–90%).

The latest test, Mo-7, was performed with an initial Mo/Cs molar ratio of 5 but with a total mass of powders less than in tests Mo-1 and Mo-2 (5.5 g for Mo-7 vs about 9.5 g for Mo-1 and Mo-2, Table 2). This test aimed to determine any mass powder effect on the release of gaseous iodine. The mass of gaseous iodine released was increased (x 1.76 the amount released in Mo-1). The reaction rate between the two compounds was then affected by the molar amount of the substance present initially. Molecular iodine was also detected in toluene. The concentration calculated from the measured absorbance in Mo-7 corresponded to 82.4% of the total amount of measured gaseous iodine.

3.2. Characteristics of transported aerosols

The transport of the aerosols was studied by:

- the analysis of the stainless steel coupons placed downstream the crucible (weighed and analysed by Raman microspectrometry);
- the elemental characterisation of the particles collected on the filters (ICP-MS);
- the determination of the ratio particles/gas between elemental amounts collected on the filter and trapped in the scrubber;
- the number size distribution monitored by SMPS and ELPI during the tests.

After the tests performed in Ar/H_2O atmosphere, the oxidation of the coupons could be clearly identified by the presence of compounds characterized by Gardiner's study on the stainless steel oxidation at 650 °C [23]. Consequently, the mass gain of the coupons could, with difficulty, be attributed to the mass of the deposited/condensed material. However, hydrates of molybdenum oxide ($MoO_3 \cdot xH_2O$) were identified on the basis of the work published by Seguin et al. [24], in addition to caesium iodide [25]. The analysis of the stainless steel coupons placed downstream the crucible during tests in Ar/Air atmosphere revealed the same information as from the tests performed under Ar/H_2O, that is to say the oxidation of the stainless steel. Caesium iodide was characterized but no molybdenum species were detected, probably because of the small amount of deposited/condensed species.

On the filters, lower mass concentrations of particles were collected when molybdenum was present in the crucible (Table 3). More particles were transported through the facility during the heating of caesium iodide. This observation could mostly be explained by the reaction between caesium iodide and molybdenum trioxide leading to the formation of caesium molybdates, less volatile species than caesium iodide. Upstream the dilution stages, the deposition process of caesium molybdates could be increased. The vaporisation rate has been calculated from the loss of mass of powder mixture in the crucible after the test and the duration of the test (Table 3). It showed a higher vaporisation rate in presence of molybdenum and in the Ar/Air atmosphere.

The mass concentration of molybdenum and caesium on the filter increased as the initial Mo/Cs molar ratio was increased in the crucible. As measured in gaseous phase, the mass concentration of iodine in particles was the highest when Mo/Cs = 1.6. The Cs/I molar ratio on the filter was lower than 1 (Table 3), except for the test Mo-1 and Mo-7. Looking at the tests performed in Ar/H_2O atmosphere, the Mo/Cs molar ratio calculated on the filter was lower than the one initially calculated in the crucible. An opposite behaviour was noticed in the Ar/Air atmosphere; the Mo/Cs ratio calculated on the filter was higher than the one initially calculated in the crucible. This would suggest that higher amount of molybdenum was released in Ar/Air atmosphere.

By comparing the ratios between the amount of element collected on the filters and the ones trapped in the liquid scrubbers, it can be highlighted that iodine reached the sampling lines mostly under gaseous form; while caesium and molybdenum reached the sampling lines as particles in presence of molybdenum.

Based on these observations, the presence of molybdenum in the crucible tended to decrease the overall release of caesium and to increase the gaseous iodine release. The higher vaporisation rate calculated for the tests Mo-1 to Mo-7, in comparison with the caesium iodide vaporisation tests (CsI-A and CsI-D) would be explained by the higher vaporisation of molybdenum.

The particle number concentrations of the tests Mo-1, Mo-3 and Mo-5 were lower than for the test performed with only caesium iodide CsI-A (Table 3). The mass concentrations of particles sampled on the filter corroborated that less particles were transported to the sampling lines, or below 500 °C, when molybdenum was present. From these tests, no correlation can be made between the initial Mo/Cs molar ratio in the crucible and the CMD (Fig. 3). In the experimental conditions studied in the present work, the SMPS measurements provided generally higher particle number concentration than the ELPI measurements. This difference can be explained by the fact that the ELPI particle mobility diameter is aerodynamic diameter and the SMPS particle diameter is the electrical mobility diameter. ELPI constantly measured lower particle number concentration than SMPS when the majority of the produced particles are in a size range of 30–80 nm. In that range, SMPS detects particles more efficiently than ELPI. This is highlighted by test CsI-D, for which the measured CMD was 253 nm; in this case, the SMPS measurements provided lower particle number concentration than the ELPI measurements. The test performed in Ar/Air with a molar Mo/Cs ratio of 3 (Mo-6) showed the smallest CMD. However, as the observation of smaller CMD in Ar/Air was not a generality in the tests, no correlation can be made between the atmosphere composition and the CMD.

The particle number size distribution and the mass concentration recorded for Mo-7 were in agreement with those measured for tests with higher amounts of powders (Table 3). While it seems that the initial mass had no effect on the transport of caesium, the measured amount of iodine and molybdenum were affected. The decrease of the transported mass of molybdenum (particles) when the total amount of powders was decreased (from 9.5 g to 5.5 g) could be expected as the mass of molybdenum trioxide was decreased as well (from 7.011 g to 4.027 g).

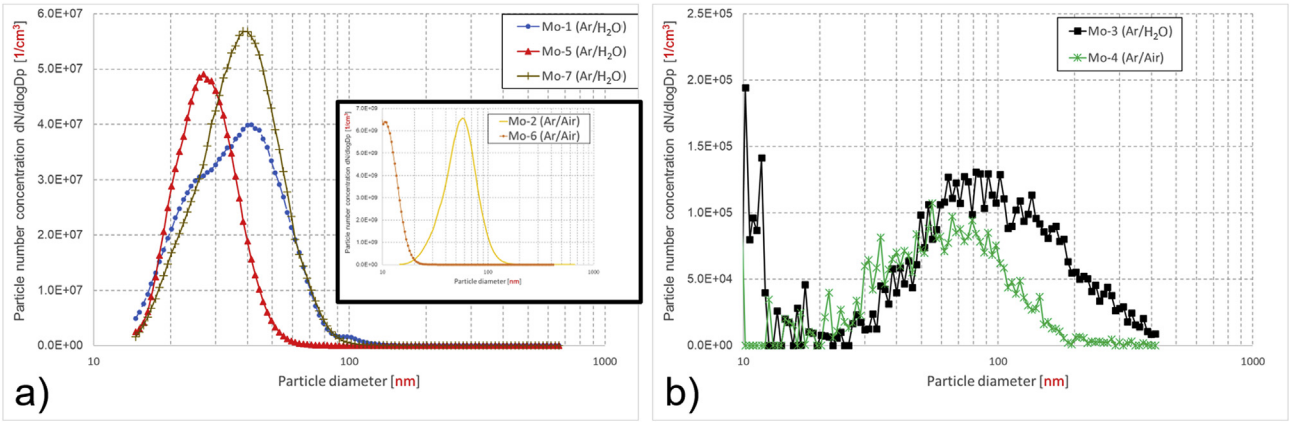

Fig. 3. Number concentration of particles transported through the facility as a function of the particle electrical mobility diameter recorded with SMPS. Dp represents particle diameter. The curves represent mean values for several scans.

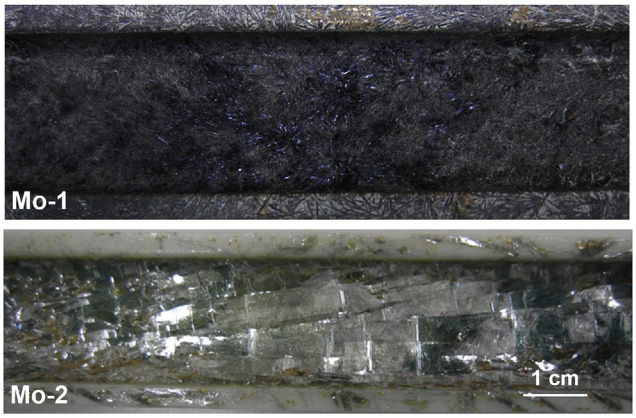

Fig. 4. Picture the residues in the alumina crucible after experiments conducted between caesium iodide and molybdenum trioxide (Mo/Cs = 5) under Ar/H_2O (Mo-1) and Ar/Air (Mo-2) carrier gas.

3.3. Nature of the residues in the crucible

At the studied temperature, the molybdenum trioxide was in solid form (m.p.[1] 795 °C) and caesium iodide in liquid form (m.p. 621 °C) [26]. Consequently, either the liquid reactant diffused onto the powder grains surface leading to a solid/liquid reaction or the solid powder dissolved into the liquid caesium iodide, leading to a liquid/liquid reaction.

The tests Mo-1, Mo-3 and Mo-5 were performed under similar gas composition (Ar/H_2O), with similar initial mass of caesium iodide but with different Mo/Cs molar ratios (from 1.6 to 5). In the crucible, the remaining material after the tests exhibited different appearances and different molecular compositions (Fig. 4). In the Mo-1 crucible, agglomerates of parallelepipedic-like crystals were identified mostly as a mixture of orthorhombic molybdenum trioxide (α-MoO_3) and caesium iodide. The Mo-3 crucible showed a dark crust associated with the caesium molybdate ($Cs_2Mo_3O_{10}$), caesium iodide and molybdenum trioxide (Table 3). The Raman spectra of the dark and purple crust remaining in the Mo-5 crucible were clearly assigned in comparison with the reference spectra to caesium molybdate $Cs_2Mo_5O_{16}$ [27] and caesium iodide.

The tests Mo-2, Mo-4 and Mo-6 were performed under similar gas composition (Ar/Air), with similar initial mass of caesium iodide but with different Mo/Cs molar ratios (from 1.6 to 5). In the Mo-2 crucible, under Ar/Air atmosphere, the remaining material looked like shattered bluish glass (Fig. 4). Despite some bands of the spectra exhibited shifts close to those of molybdenum trioxide (276 cm^{-1}, 822 cm^{-1} and 994 cm^{-1}), others cannot be attributed to this species. Composition of the remaining material in the crucible Mo-2 was then unidentified. In the Mo-4 crucible, white and yellow crystals were observed and again were not identified. Finally, the Raman spectra of the shattered glass from the test Mo-6 did not exhibit any peak except the alumina coming from the crucible. The most probable reason was the very low amount of residue remaining in the crucible after the test (Table 3).

Concerning the test Mo-7, it can be said that the Raman spectra of the remaining material in the crucible exhibited similar shifts as Mo-1 and Mo-2.

3.4. Observations on the variation of oxygen partial pressure inside the system

The oxygen partial pressure was on-line measured during the tests. Two blank tests were performed under Ar/H_2O (condition A) and Ar/Air (condition D) atmospheres, running the blank tests similarly to the tests. The only difference was that the crucible was empty (without any precursor material inside). The tests were performed in order to assess the oxygen pressure related to these two different atmospheres (Fig. 5). The measured difference between the 2 atm compositions was noticeable. When air was present, the oxygen partial pressure was higher ($1.7 \cdot 10^{-12}$ atm in average for Ar/H_2O and $3 \cdot 10^{-2}$ atm for Ar/Air), which was expected considering the high amount of oxygen in air. During the temperature recording, the steam fraction in the atmosphere, measured with FTIR, remained constant.

When the MoO_3/CsI mixture was used as a precursor in the crucible, the measured oxygen partial pressure changed. Although the oxygen partial pressure increased in the presence of molybdenum oxide in Ar/H_2O atmosphere (from 10^{-12} atm to 10^{-4} atm), the difference in Ar/Air atmosphere was not significant (Fig. 5). However, no change in the oxygen partial pressure was observed when the initial Mo/Cs molar ratio was changed; the values recorded for Mo-1 and Mo-3 (and for Mo-2 and Mo-4) were similar.

The composition of the carrier gas (and its impurities) defines the overall partial pressure of oxygen above the powdery precursor mixture. This oxygen partial pressure, in equilibrium with the precursor, changes the deviation in stoichiometry. Therefore,

[1] m. p.: melting point.

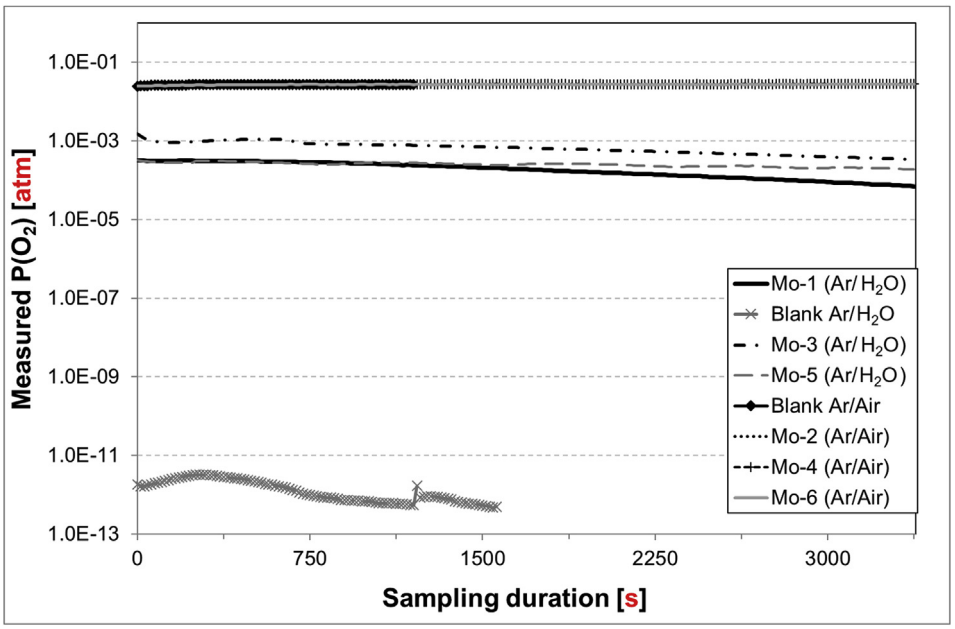

Fig. 5. Evolution of the oxygen partial pressure and temperature at the location of the crucible, recorded with the MicroPoas probe. The values of Blank Ar/Air, Mo-2, Mo-4 and Mo-6 are overlapping. The measurement times for the blanks (Blank Ar/H_2O and Blank/Air) were shorter than the measurement time of the tests.

oxidation or reduction reactions may happen, which are accompanied by the consumption or release of oxygen. If the amount of oxygen is significant, it can cause variation in the overall oxygen partial pressure of the gas in equilibrium with the precursor.

4. Discussion

4.1. Comparison with previous tests performed with caesium iodide and molybdenum

The present work was compared with previous studies performed in condensed phase. Previous work has been performed at VTT by Kalilainen et al. on the reaction between metallic molybdenum (Mo) and caesium iodide [10] and molybdenum oxide (MoO_3) and caesium iodide [5].

The tests described in Ref. [5] were performed under 3 atm compositions (100% Ar), (91% Ar – 6% H_2O – 3% H_2) and (82% Ar – 6% H_2O – 12% H_2) with molybdenum trioxide (3.75 g) and caesium iodide (1.25 g) heated to 650 °C (set point temperature). The gaseous iodine was measured to represent 99%, 48% and 7% of the total amount of iodine (gaseous and particles species) in the sampling line, respectively, for the (100% Ar), (91% Ar – 6% H_2O – 3% H_2) and (82% Ar – 6% H_2O – 12% H_2) atmosphere [5]. For the similar initial Mo/Cs molar ratio (Mo/Cs~5), despite the highest percentage of gaseous iodine was measured in the pure argon atmosphere [5], a trend can be drawn from lowest oxygen potential condition (82% Ar – 6% H_2O – 12% H_2) to highest (86.7% Ar - 13.3% Air) (Fig. 6).

The tests with metallic molybdenum powder were performed with an initial Mo/Cs molar ratio of 8, which was higher than the Mo/Cs molar ratio used in the tests performed with molybdenum trioxide (0 < Mo/Cs < 5). The tests described in Ref. [10] were performed under 3 atm compositions (90% Ar - 10% H_2O), (88.3% Ar – 10% H_2O – 2.7% H_2) and (79.2% Ar – 10% H_2O – 10.8% H_2) with molybdenum (7.5 g) and caesium iodide (2.5 g) heated to 650 °C (set point temperature). The mass of powder in the crucible increased by 1 g (initial weight was 10 g). This weight increase was explained by the reaction between the water vapour and the metallic molybdenum powder. The fraction of released gaseous iodine was higher when the precursor was molybdenum trioxide. The gaseous iodine was measured to represent 65%, 38% and 11% of the total amount of iodine (gaseous and particles species) in the sampling line, respectively, for the (90% Ar – 10% H_2O), (88.3% Ar – 10% H_2O – 2.7% H_2) and (79.2% Ar – 10% H_2O – 10.8% H_2) atmosphere [10]. The reaction between metallic molybdenum and caesium iodide (Mo+CsI) appeared consequently less effective in forming non-condensable iodine than the reaction between molybdenum trioxide and caesium iodide (MoO_3 + CsI).

As previously pointed out by Sunder in nuclear fuel [28], the iodine volatility is linked to the molybdenum oxidation state. Despite that the work was performed to understand the behaviour of iodine in nuclear fuel, a parallel can be made with the present work. The experimental results obtained by Sunder have shown that molybdenum oxidation below the +IV oxidation state (i.e. oxidation state in molybdenum dioxide (MoO_2)) did not increase the volatility of the iodine present in fuel. If the molybdenum oxidation proceeded to the molybdenum trioxide stage, the effect on iodine volatility was observed. The study carried out by Di Lemma et al. [29] by vaporisation of caesium iodide and metallic molybdenum in air (molar Mo/Cs close to 5) corroborated the kinetic effect that an oxidizing environment (oxygen potential 0.21 atm) has on the reaction between molybdenum and caesium iodide:

$$2CsI(s) + Mo(s) + 2O_2 = Cs_2MoO_4(s) + I_2(g)$$

The results of Grégoire et al. [5] have also underlined the effect of the molybdenum oxidation state on the transport of gaseous iodine. In reducing conditions, the initial molybdenum trioxide was suspected to be reduced into molybdenum dioxide. Concurrently, the amount of gaseous iodine was observed to be lower than in oxidizing conditions.

These results confirmed that the molecular form of molybdenum entering the primary circuit during a severe accident has an effect on its reactivity, and consequently on the transport of iodine.

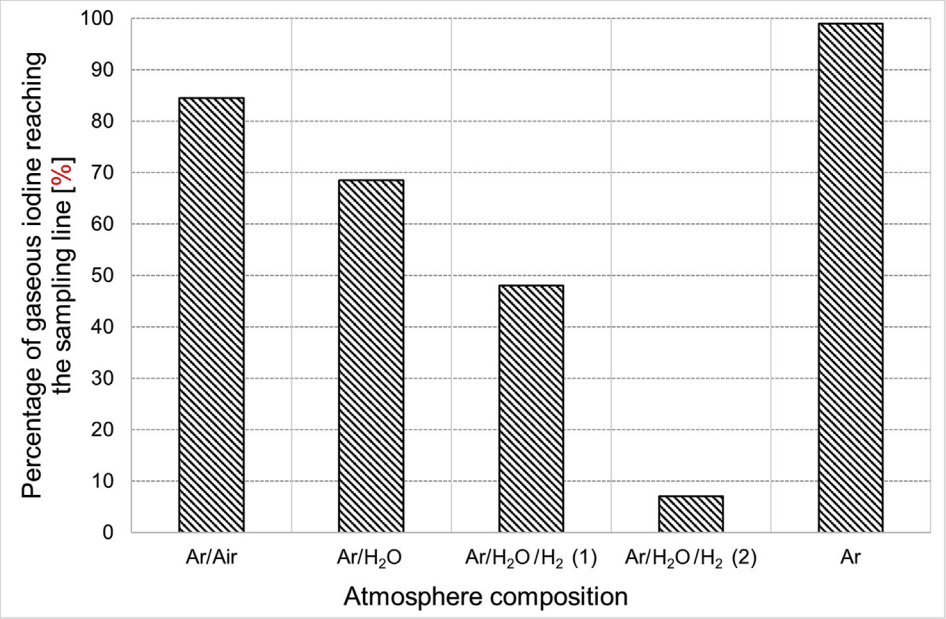

Fig. 6. Percentage of gaseous iodine reaching the sampling line calculated from the ICP-MS measurements according to the atmosphere composition.

Table 4
Mole fractions of the gaseous species (calculated with mole fraction > 10^{-6}) formed when heating the precursors at 700 °C in Condition A (86.7% Ar – 13.3% H_2O) and Condition D (86.7% Ar – 13.0% Air), calculated in chemical equilibrium with Thermfact and GTT-Technologies FactSage 5.5

700 °C	CsI		Mo/Cs = 1.6		Mo/Cs = 3		Mo/Cs = 5		Mo/Cs = 5 (less powder)	
	A	D	A	D	A	D	A	D	A	D
MoO_2I_2(g)	N/A	N/A	$6.43\cdot10^{-1}$	$3.43\cdot10^{-1}$	$5.95\cdot10^{-1}$	$6.01\cdot10^{-1}$	$6.65\cdot10^{-1}$	$3.78\cdot10^{-1}$	$5.98\cdot10^{-1}$	$6.00\cdot10^{-1}$
Mo_3O_9(g)	N/A	N/A	$<10^{-6}$	$<10^{-6}$	$<10^{-6}$	$1.34\cdot10^{-5}$	$3.10\cdot10^{-4}$	$2.83\cdot10^{-4}$	$2.84\cdot10^{-5}$	$2.80\cdot10^{-5}$
CsOH(g)	$9.78\cdot10^{-4}$	N/A	$<10^{-6}$	N/A	$<10^{-6}$	N/A	$<10^{-6}$	N/A	$<10^{-6}$	N/A
Cs_2I_2(g)	$8.77\cdot10^{-1}$	$8.78\cdot10^{-1}$	$9.84\cdot10^{-3}$	$7.93\cdot10^{-3}$	$3.15\cdot10^{-5}$	$<10^{-6}$	$<10^{-6}$	$<10^{-6}$	$<10^{-6}$	$<10^{-6}$
CsI(g)	$1.21\cdot10^{-1}$	$1.22\cdot10^{-1}$	$1.80\cdot10^{-3}$	$1.45\cdot10^{-3}$	$4.49\cdot10^{-5}$	$<10^{-6}$	$<10^{-6}$	$<10^{-6}$	$<10^{-6}$	$<10^{-6}$
Mo_4O_{12}(g)	N/A	N/A	$<10^{-6}$	$<10^{-6}$	$<10^{-6}$	$9.97\cdot10^{-6}$	$3.82\cdot10^{-4}$	$3.48\cdot10^{-4}$	$2.68\cdot10^{-5}$	$2.64\cdot10^{-5}$
I(g)	$8.52\cdot10^{-4}$	$4.05\cdot10^{-6}$	$4.80\cdot10^{-2}$	$6.27\cdot10^{-2}$	$3.06\cdot10^{-2}$	$3.04\cdot10^{-2}$	$4.52\cdot10^{-2}$	$6.04\cdot10^{-2}$	$3.10\cdot10^{-2}$	$3.09\cdot10^{-2}$
HI(g)	$1.24\cdot10^{-4}$	N/A	$2.05\cdot10^{-2}$	N/A	$9.13\cdot10^{-3}$	N/A	$3.01\cdot10^{-3}$	N/A	$2.64\cdot10^{-3}$	N/A
I_2(g)	$1.08\cdot10^{-6}$	$<10^{-6}$	$2.77\cdot10^{-1}$	$5.85\cdot10^{-1}$	$3.65\cdot10^{-1}$	$3.69\cdot10^{-1}$	$2.86\cdot10^{-1}$	$5.61\cdot10^{-1}$	$3.67\cdot10^{-1}$	$3.69\cdot10^{-1}$
HIO(g)	$<10^{-6}$	N/A	$4.72\cdot10^{-6}$	N/A	$4.92\cdot10^{-6}$	N/A	$2.75\cdot10^{-5}$	N/A	$1.76\cdot10^{-5}$	N/A
Mo_5O_{15}(g)	N/A	N/A	$<10^{-6}$	$<10^{-6}$	$<10^{-6}$	$<10^{-6}$	$3.04\cdot10^{-5}$	$2.77\cdot10^{-5}$	$1.45\cdot10^{-6}$	$1.43\cdot10^{-6}$
$O_2Mo(OH)_2$	N/A	N/A	$2.44\cdot10^{-5}$	N/A	$2.64\cdot10^{-5}$	N/A	$8.02\cdot10^{-4}$	N/A	$3.34\cdot10^{-4}$	N/A

4.2. Analysis with thermochemical equilibrium calculations

Calculations were made at 700 °C (Table 4) as it was the temperature measured above the crucible during the tests (Fig. 2). The calculations were done by setting the caesium iodide amount to 0.96 mol and to adjust the molybdenum trioxide amount by keeping the molar Mo/Cs ratio. For the Mo-7 test condition, the initial amount of caesium iodide was set to 0.55 mol. The pressure was fixed to 1 atm.

It is worth to remind that, in the EXSI-PC facility, the dilutors were used in order to limit the chemical and aerosol processes during the cooling down, and then, gather data about what was released from the crucible, freeing the results from the possible recombination or deposition processes during the transport to the sampling line. In order to reproduce roughly the transport of the species from the crucible to the sampling line, calculations were performed at 25 °C started with the composition of the gaseous phase determined at 700 °C (Table 6). The results of the thermochemical equilibrium calculations at 700 °C and 25 °C should then be taken as boundary cases.

At 700 °C, caesium iodide vaporised mostly into gaseous caesium iodide and its dimer (>99% of the total iodine species in gaseous phase, see Table 4). The vaporisation in Ar/H_2O atmosphere led to the formation of low amount of non-condensable[2] iodine species (HI, I_2, HIO and I) which were not predicted in Ar/Air atmosphere. This is due to the reaction between caesium iodide and steam, producing caesium hydroxide and non-condensable iodine species.

In the presence of molybdenum oxide, the amount of non-condensable iodine species, particularly under molecular iodine form, was enhanced - both in steam and air atmospheres (Table 4). The non-condensable iodine fraction reached 30–35% in presence of molybdenum trioxide in steam atmosphere and up to 60% in air compared to less than 0.1% for caesium iodide vaporisation. Experimentally, the fraction of gaseous iodine was also increased in the presence of molybdenum and was assessed to be higher than 50% and higher than 85% in air (Table 3). The higher experimental value compared to the calculated ones can be attributed to the

[2] In the present paper, the term "non-condensable iodine species" is used to describe iodine species condensing at temperatures lower than 150 °C (HI, I_2, HIO and I), by opposition to condensable iodine species, such caesium iodide (CsI) and molybdenum oxyiodide (MoO_2I_2), condensing at temperatures higher than 150 °C.

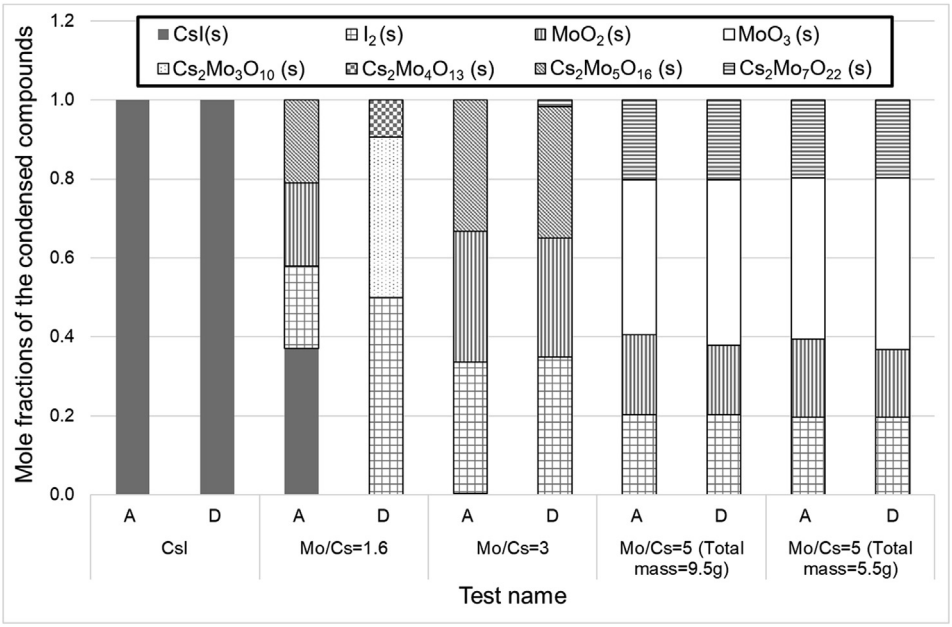

Fig. 7. Mole fractions of the condensed compounds (calculated with mole fraction > 10^{-6}) formed when heating CsI and MoO_3 (Mo/Cs = 1.6, Mo/Cs = 3 and Mo/Cs = 5) at 700 °C in Condition A (86.7% Ar − 13.3% H_2O) and Condition D (86.7% Ar − 13.0% Air), calculated in chemical equilibrium with Thermfact and GTT-Technologies FactSage 5.5.

deposition of the particles and condensation of "condensable iodine species" in the facility from the crucible to the sampling line, resulting in increasing the fraction of experimentally measured gaseous species. As measured experimentally, for the two studied atmosphere compositions, the major gaseous iodine species was molecular iodine.

At the thermochemical equilibrium, with the increase of the initial Mo/Cs molar ratio, all the gaseous caesium iodide tended to react and was not present in gaseous phase anymore. Experimentally, the fraction of gaseous iodine was higher in the test with the lowest Mo/Cs ratio. This difference, between the chemical equilibrium calculation and the experiment, can be interpreted either as a defect in the measurement, as the tests Mo/Cs = 3 and Mo/Cs = 5 followed an increasing trend in the transport of non condensable iodine species, or an effect due to the lower initial mass of molybdenum present in the crucible (only 2.2 g for Mo/Cs = 1.6). The thermochemical equilibrium calculations, performed with Mo/Cs molar ratio of 5 but having an initial amount of material divided by 2, showed the disappearance in gaseous phase that of some molybdenum species, such as Mo_5O_{15} but also an increase of the molecular iodine fraction in Ar/H_2O.

By increasing the amount of molybdenum trioxide initially

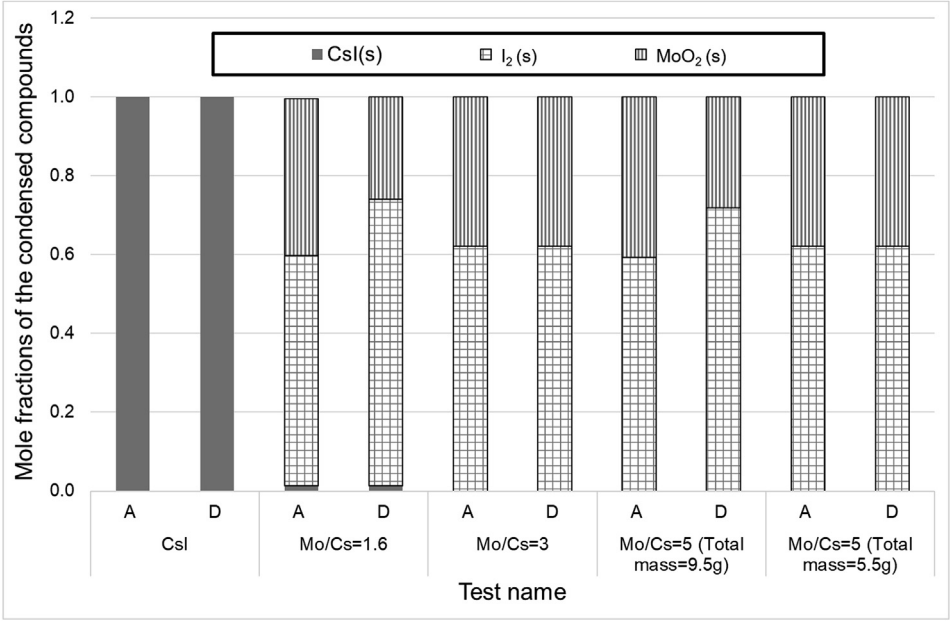

Fig. 8. Mole fractions of the condensed compounds (calculated with mole fraction > 10^{-6}) formed when heating CsI and MoO_3 (Mo/Cs = 1.6, Mo/Cs = 3 and Mo/Cs = 5) at 25 °C in Condition A (86.7% Ar − 13.3% H_2O) and Condition D (86.7% Ar − 13.0% Air), calculated in chemical equilibrium with Thermfact and GTT-Technologies FactSage 5.5.

Table 5
Oxygen partial pressure (in atm) calculated when heating the precursors at 700 °C in Condition A (86.7% Ar – 13.3% H_2O) and Condition D (86.7% Ar – 13.0% Air), in chemical equilibrium with Thermfact and GTT-Technologies FactSage 5.5

700 °C	Blank	CsI	Mo/Cs = 1.6	Mo/Cs = 3	Mo/Cs = 5
Ar/Air	$2.30\cdot10^{-2}$	$2.29\cdot10^{-2}$	$1.66\cdot10^{-12}$	$1.62\cdot10^{-11}$	$2.43\cdot10^{-9}$
Ar/H_2O	$1.86\cdot10^{-8}$	$5.70\cdot10^{-12}$	$1.29\cdot10^{-13}$	$2.00\cdot10^{-13}$	$2.04\cdot10^{-10}$

present in the crucible, the thermochemical equilibrium calculated an increase of the amount of molybdenum trioxide $(MoO_3)_n$ polymers in gaseous phase (Table 4).

The calculations indicated the presence of molybdenum oxyiodide (MoO_2I_2) in the presence of steam. Its presence has been explained in the literature for high temperature (above 650 °C [30]), as the result of reaction between iodine, acting as a transport agent, and molybdenum dioxide (MoO_2) [30,31].

In order to interpret the condensed species identified experimentally as residue in the crucible (Table 3), thermochemical equilibrium calculations were performed at 700 °C (Fig. 7) and 25 °C (Fig. 8).

At 700 °C, the results of the mixture heating (Mo/Cs = 1.6) led to the formation of caesium molybdate $Cs_2Mo_3O_{10}$. Some caesium iodide remained unreacted and molybdenum trioxide has turned to molybdenum dioxide in Ar/H_2O atmosphere. With the increase of the Mo/Cs molar ratio in the crucible, the caesium iodide totally disappeared and caesium molybdates containing higher percentage of molybdenum ($Cs_2Mo_5O_{16}$ and $Cs_2Mo_7O_{22}$) were formed. In addition, some molybdenum trioxide remained unreacted.

Experimentally, caesium molybdates were also identified. However differences in the species were observed. In addition, remaining of caesium iodide in the crucible after the experiments were almost always measured, contrary to the thermochemical equilibrium calculations, which underline the full reaction of caesium iodide with the increase of molybdenum trioxide amount in the crucible.

The results of the calculations performed at 25 °C started with the composition of the gaseous phase determined at 700 °C (Table 6) showed the presence of molecular iodine calculated for all the mixture tests in gaseous phase but also in condensed phase (Fig. 8). For the tests with molybdenum trioxide, the main condensed species were molecular iodine and molybdenum dioxide. The iodine species represented the gaseous phase majority for the tests with molybdenum.

The thermochemical equilibrium calculations also allowed comparing the evolution of the oxygen partial pressure. The thermochemical equilibrium calculations were performed in order to identify the major species, not to determine their exact quantity, so the fugacity cannot be directly compared to the experimentally measured ones. However, it was possible to compare the evolution between the different calculations (Table 5). As observed experimentally for the measurements of the blank tests, the partial pressure was higher in the Ar/Air atmosphere than in Ar/H_2O atmosphere. From the calculated results, the increase of the oxygen partial pressure, due to the presence of molybdenum trioxide in the crucible, in steam condition was not observed, contrary to what has been measured experimentally. However, the oxygen partial pressure was calculated to increase as the initial Mo/Cs increased.

5. Conclusion

The study was specifically focused on investigating reactions, which could happen from the deposits in the reactor coolant system.

The influence of molybdenum on the release of gaseous iodine from a condensed reaction between molybdenum trioxide and caesium iodide has been confirmed. The present results supplement the previous published work, notably by providing information concerning the role of the initial Mo/Cs molar ratio and the reactions in presence of air.

The studied initial Mo/Cs molar ratios (Mo/Cs = 1.6; 3 and 5) expanded the matrix of previously studied conditions. However, the tests showed unexpected results by measuring higher amount of released gaseous iodine for the smaller Mo/Cs. Further tests are required in order to confirm this observation. First hypothesis questioned the role of the initial mass of powders in the crucible but other suggestions are under consideration.

As a consistent observation, for all the studied Mo/Cs, the release of gaseous iodine was higher when the oxygen partial pressure was higher (*i.e.* for Ar/Air atmosphere). The experimental results supported the previously formulated conclusion [5] and recalled the role of the molybdenum oxidation state on the gaseous iodine formation. Gaseous molecular iodine was clearly identified as the main gaseous iodine species formed during the reaction (>50%).

Several caesium molybdates were found in the crucible after the tests, confirming that the reaction between caesium and molybdenum was the reason for the observed formation of gaseous iodine.

The experimental results were analysed by comparison with thermochemical equilibrium calculation results. The experimental measurements were mostly in accordance with the thermochemical equilibrium calculations, looking at the role of the atmosphere composition.

In order to understand the observed phenomena, it is suggested to first confirm the observed results by repeating the tests, and then include modelization of the process. For instance, for the solid structure, shrinking particle, product layer and grain models are usually proposed to explain condensed-phase reactions. Discussing the observed experimental data with results from one of those models could provide more information.

In addition, as previously pointed out by Gouëllo et al. [32] in similar study investigating boron and caesium iodide reactions, and by McFarlane et al. [7], the initial Cs/I molar ratio is also an relevant parameter which will influence the release of gaseous iodine. Then,

Table 6
Mole fractions of the gaseous species (calculated with mole fraction > 10^{-6}) formed when cooling down to 25 °C the composition of the gaseous phase determined at 700 °C in Condition A (86.7% Ar – 13.3% H_2O) and Condition D (86.7% Ar – 13.0% Air), calculated in chemical equilibrium with Thermfact and GTT-Technologies FactSage 5.5

25 °C	CsI		Mo/Cs = 1.6		Mo/Cs = 3		Mo/Cs = 5		Mo/Cs = 5 (less powder)	
	A	D	A	D	A	D	A	D	A	D
Cs_2I_2(g)	$1.38\cdot10^{-1}$	$<10^{-6}$	$<10^{-6}$	$<10^{-6}$	$<10^{-6}$	$<10^{-6}$	$<10^{-6}$	$<10^{-6}$	$<10^{-6}$	$<10^{-6}$
CsI(g)	$1.11\cdot10^{-3}$	$<10^{-6}$	$<10^{-6}$	$<10^{-6}$	$<10^{-6}$	$<10^{-6}$	$<10^{-6}$	$<10^{-6}$	$<10^{-6}$	$<10^{-6}$
I(g)	$6.31\cdot10^{-1}$	$<10^{-6}$	$<10^{-6}$	$<10^{-6}$	$<10^{-6}$	$<10^{-6}$	$<10^{-6}$	$<10^{-6}$	$<10^{-6}$	$<10^{-6}$
HI(g)	$3.03\cdot10^{-2}$	N/A	$6.06\cdot10^{-1}$	N/A	$6.06\cdot10^{-1}$	N/A	$1.80\cdot10^{-6}$	N/A	$5.95\cdot10^{-1}$	N/A
I_2(g)	$2.56\cdot10^{-6}$	1.00	$3.94\cdot10^{-1}$	1.00	$3.94\cdot10^{-1}$	1.00	1.00	1.00	$4.05\cdot10^{-1}$	1.00
HIO(g)	$2.00\cdot10^{-1}$	N/A	$<10^{-6}$	N/A	$<10^{-6}$	N/A	$<10^{-6}$	N/A	$<10^{-6}$	N/A

it is obviously proposed to look into the behaviour of iodine in the conditions of the present work with an initial Cs/I molar ratio higher than one.

Acknowledgments

This work was supported by the Finnish Research Programme on Nuclear Power Plant Safety (SAFIR2018).

Appendix A. Supplementary data

Supplementary data to this article can be found online at https://doi.org/10.1016/j.net.2020.01.029.

References

[1] T.-M.-D. Do, S. Sujatanond, T. Ogawa, Behavior of cesium molybdate, Cs2MoO4 , in severe accident conditions. (1) partitioning of Cs and Mo among gaseous species, J. Nucl. Sci. Technol. 55 (2018) 348–355, https://doi.org/10.1080/00223131.2017.1397560.

[2] J.-P. Van Dorsselaere, A. Auvinen, D. Beraha, P. Chatelard, L.E. Herranz, C. Journeau, W. Klein-Heßling, I. Kljenak, A. Miassoedov, S. Paci, R. Zeyen, Recent severe accident Research synthesis of the major outcomes from the SARNET network, Nucl. Eng. Des. 291 (2015) 19–34, https://doi.org/10.1016/j.anucene.2016.02.014.

[3] G. Ducros, Y. Pontillon, P.P. Malgouyres, Synthesis of the VERCORS experimental programme: separate-effect experiments on fission product release, in support of the phébus-FP programme, Ann. Nucl. Energy 61 (2013) 75–87, https://doi.org/10.1016/j.anucene.2013.02.033.

[4] A.-C. Grégoire, T. Haste, Material release from the bundle in Phébus FP, Ann. Nucl. Energy 61 (2013) 63–74, https://doi.org/10.1016/j.anucene.2013.02.037.

[5] A.-C. Grégoire, J. Kalilainen, F. Cousin, H. Mutelle, L. Cantrel, A. Auvinen, T. Haste, S. Sobanska, Studies on the role of molybdenum on iodine transport in the RCS in nuclear severe accident conditions, Ann. Nucl. Energy 78 (2015) 117–129, https://doi.org/10.1016/j.anucene.2014.11.026.

[6] M. Gouëllo, H. Mutelle, F. Cousin, S. Sobanska, E. Blanquet, Analysis of the iodine gas phase produced by interaction of CsI and MoO3 vapours in flowing steam, Nucl. Eng. Des. 263 (2013) 462–472, https://doi.org/10.1016/j.nucengdes.2013.06.016.

[7] J. McFarlane, J.C. Wren, R.J. Lemire, Chemical speciation of iodine source term to containment, Nucl. Technol. 138 (2002) 162–178. http://www.osti.gov/energycitations/product.biblio.jsp?osti_id=20826755.

[8] N. Girault, C. Fiche, A. Bujan, J. Dienstbier, Towards a better understanding of iodine chemistry in RCS of nuclear reactors, Nucl. Eng. Des. 239 (2009) 1162–1170, https://doi.org/10.1016/j.nucengdes.2009.02.008.

[9] K. Mueller, S. Dickinson, C. de Pascale, N. Girault, L. Herranz, F. De Rosa, G. Henneges, J. Langhans, C. Housiadas, V. Wichers, A. Dehbi, S. Paci, F. Martin-Fuertes, I. Turcu, I. Ivanov, B. Toth, G. Horvath, Validation of severe accident codes on the phebus fission product tests in the framework of the PHEBEN-2 project, Nucl. Technol. 163 (2008) 209–227, https://doi.org/10.13182/NT08-A3982.

[10] J. Kalilainen, T. Kärkelä, R. Zilliacus, U. Tapper, A. Auvinen, J. Jokiniemi, Chemical reactions of fission product deposits and iodine transport in primary circuit conditions, Nucl. Eng. Des. 267 (2014) 140–147, https://doi.org/10.1016/j.nucengdes.2013.11.078.

[11] J. Sugimoto, M. Kajimoto, K. Hashimoto, K. Soda, Short Overview on the Definitions and Significance of the Late Phase Fission Product Aerosol/Vapour Source, 1994. Tokai- Mura (Japan).

[12] G. Katata, M. Chino, T. Kobayashi, H. Terada, M. Ota, H. Nagai, M. Kajino, R. Draxler, M.C. Hort, A. Malo, T. Torii, Y. Sanada, Detailed source term estimation of the atmospheric release for the Fukushima Daiichi nuclear power station accident by coupling simulations of an atmospheric dispersion model with an improved deposition scheme and oceanic dispersion model, Atmos. Chem. Phys. 15 (2015) 1029–1070, https://doi.org/10.5194/acp-15-1029-2015.

[13] E.H.P. Cordfunke, R.J.M. Konings, Chemical interactions in water-cooled nuclear fuel: a thermochemical approach, J. Nucl. Mater. 152 (1988) 301–309, https://doi.org/10.1016/0022-3115(88)90341-8.

[14] D. Cubicciotti, B.R. Sehgal, Vapor transport of fission products in postulated severe light water reactor accidents, Nucl. Technol. 65 (1984) 266–291, https://doi.org/10.13182/NT84-A33411.

[15] M. Gouëllo, J. Hokkinen, T. Kärkelä, A. Auvinen, A scoping study of chemical behaviour of caesium iodide in presence of boron in condensed phase (650 °C and 400 °C) under primary circuit conditions, Nucl. Technol. 203 (2018) 66–84, https://doi.org/10.1080/00295450.2018.1429111.

[16] W. Klein-Heßling, M. Sonnenkalb, D. Jacquemain, B. Clément, E. Raimond, H. Dimmelmeier, G. Azarian, G. Ducros, C. Journeau, L.E. Herranz Puebla, A. Schumm, A. Miassoedov, I. Kljenak, G. Pascal, S. Bechta, S. Güntay, M.K. Koch, I. Ivanov, A. Auvinen, I. Lindholm, Conclusions on severe accident Research priorities, Ann. Nucl. Energy (2014), https://doi.org/10.1016/j.anucene.2014.07.015.

[17] J. Kalilainen, Chemical Reactions on Primary Circuit Surfaces and Their Effects on Fission Product Transport in a Severe Nuclear Accident, Aalto University, 2010.

[18] G. Ducros, Y. Pontillon, P.-P. Malgouyres, P. Taylor, Y. Dutheillet, Ruthenium release at high temperature from irradiated PWR fuels in various oxidising conditions; main findings from the VERCORS program, in: Nucl. Energy New Eur. 2005, Nuclear Society of Slovenia, Bled (Slovenia), Slovenia, 2005, pp. 34.1–34.14.

[19] M. Gouëllo, J. Kalilainen, T. Kärkelä, A. Auvinen, Contribution to the understanding of iodine transport under primary circuit conditions: CsI/Cd and CsI/Ag interactions in condensed phase, Nucl. Mater. Energy. 17 (2018) 259–268, https://doi.org/10.1016/J.NME.2018.11.011.

[20] T. Haste, F. Payot, P.D.W. Bottomley, Transport and deposition in the Phébus FP circuit, Ann. Nucl. Energy 61 (2013) 102–121. http://www.sciencedirect.com/science/article/pii/S0306454912004355.

[21] C.W. Bale, E. Bélisle, P. Chartrand, S.A. Decterov, G. Eriksson, K. Hack, I.-H. Jung, Y.-B. Kang, J. Melançon, A.D. Pelton, C. Robelin, S. Petersen, FactSage thermochemical software and databases — recent developments, Calphad 33 (2009) 295–311, https://doi.org/10.1016/j.calphad.2008.09.009.

[22] H.A. Benesi, J.H. Hildebrand, A spectrophotometric investigation of the interaction of iodine with aromatic hydrocarbons, J. Am. Chem. Soc. 71 (1949) 2703–2707. http://pubs.acs.org/doi/pdf/10.1021/ja01176a030.

[23] D.J. Gardiner, C.J. Littleton, K.M. Thomas, K.N. Strafford, Distribution and characterization of high temperature air corrosion products on iron-chromium alloys by Raman microscopy, Oxid. Metals 27 (1987) 57–72.

[24] L. Seguin, M. Figlarz, R. Cavagnat, J.-C. Lassègues, Infrared and Raman spectra of MoO3 molybdenum trioxides and MoO3 · xH2O molybdenum trioxide hydrates, Spectrochim. Acta Part A Mol. Biomol. Spectrosc. 51 (1995) 1323–1344, https://doi.org/10.1016/0584-8539(94)00247-9.

[25] G.C. Allen, J.W. Tyler, Chemical state and distribution of iodine deposits on 17% Cr/12% Ni steel oxidised in CO2/CH3I gas mixtures, J. Nucl. Mater. 170 (1990) 276–285, https://doi.org/10.1016/0022-3115(90)90299-3.

[26] W.M. Haynes, CRC Handbook of Chemistry and Physics : a Ready-Reference Book of Chemical and Physical Data, 92nd ed., 2011.

[27] H.A. Hoekstra, The Cs2MoO4 - MoO3 system, Inorg. Nucl. Chem. Lett. 9 (1973) 1291–1301.

[28] S. Sunder, The relationship between molybdenum oxidation state and iodine volatility in nuclear fuel, Nucl. Technol. 144 (2003) 259–273. http://cat.inist.fr/?aModele=afficheN&cpsidt=15205641.

[29] F.G. Di Lemma, J.Y. Colle, O. Beneš, R.J.M. Konings, A separate effect study of the influence of metallic fission products on CsI radioactive release from nuclear fuel, J. Nucl. Mater. 465 (2015) 499–508, https://doi.org/10.1016/j.jnucmat.2015.05.037.

[30] M. Lenz, R. Gruehn, Developments in measuring and calculating chemical vapor transport phenomena demonstrated on Cr, Mo, W, and their compounds, Chem. Rev. 97 (1997) 2967–2994.

[31] L.A. Klinkova, E.D. Skrebkova, Heterogeneous equilibrium in system MoO2-I2, Inorg. Mater. 13 (1977) 380–383.

[32] M. Gouëllo, J. Hokkinen, T. Kärkelä, A. Auvinen, A complementary study to the chemical behaviour of caesium iodide in presence of boron in condensed phase (650 °C and 400 °C) under primary circuit Conditions : differential thermal analysis and thermogravimetric studies, Nucl. Technol. 203 (2018) 85–91, https://doi.org/10.1080/00295450.2018.1430463.